Hindawi
International Transactions on Electrical Energy Systems
Volume 2022, Article ID 6017066, 11 pages
https://doi.org/10.1155/2022/6017066

Research Article

A Novel Optimal Robust Design Method for Frequency Regulation of Three-Area Hybrid Power System Utilizing Honey Badger Algorithm

Rajendra Kumar Khadanga,[1] **Smruti Ranjan Nayak**,[1] **Sidhartha Panda**,[2] **Deepa Das**,[3] **B. Rajanarayan Prusty**,[4] **and Preeti Ranjan Sahu**[5]

[1]*Department of Electrical and Electronics Engineering, Centurion University of Technology and Management, Bhubaneswar-752050, Odisha, India*
[2]*Department of Electrical Engineering, Veer Surendra Sai University of Technology, Burla-768018, Odisha, India*
[3]*Department of Electrical Engineering, Government College of Engineering, Kalahandi-766002, Kandha Bando Pala, Odisha, India*
[4]*Department of Electrical and Electronics Engineering, Alliance College of Engineering and Design, Alliance University, Bengaluru-562106, Karnataka, India*
[5]*Department of Electrical and Electronics Engineering, National Institute of Science and Technology, Berhampur-761008, Odisha, India*

Correspondence should be addressed to B. Rajanarayan Prusty; b.r.prusty@ieee.org

Received 22 August 2022; Revised 3 November 2022; Accepted 5 November 2022; Published 15 November 2022

Academic Editor: Michele De Santis

This study proposes an innovative technique for the load frequency control (LFC) of a three-area hybrid power system by putting into consideration of honey badger algorithm-based fractional order proportional integral derivative (FOPID) controller. The algorithm's veritable use is attempted by arranging a FOPID controller for the hybrid system's frequency regulation; the incredible potential of the proposed algorithm is proven. The proposed HBA-based FOPID regulator is presented by comparing its results with other current methods. It is seen that the said regulator is more viable for the frequency control contrasted with the regular regulator by considering a change in system parameters and different paces of RES penetration. It is also seen that the recommended controller is found to be more effective for load frequency control than the conventional controllers.

1. Introduction

The undertaking of load frequency control (LFC) is to affirm the frequency deviations inside a predetermined reach beyond what many would consider possible [1]. This critical problem identified with LFC is pivotal in a comprehensive planned power system to maintain the frequency within a sensible limit [2]. The literature study proves that many past investigations have been done to solve the LFC issue. The frequency regulation of a two-area interconnected power system is the focus of most ebb and flow research on LFC. Few have assessed customary energy sources, and, surprisingly, fewer have considered the effect of distributed sources on the LFC plan [3–5]. A three-area power system is used to verify the extension of a two-area power system [6–8]. However, almost no research has considered the impact of integrating various renewable energy sources in a three-area power system [9–11].

Different controllers have been proposed to deal with the LFC frequency control issue. The application of proportional integral and derivative have been used for LFC issues [12], tilt-integral-derivative controller [13], cascade tilt-integral-tilt-derivative controller [14], fractional-order PID controller [15], FPI-FPD cascade controller [16], fractional-order three-degrees-of-freedom TID controller [17], and Type-1 and Type-2 fuzzy PID controller [18–20] have also been used by the researchers. Apart from this, none of the researchers have reported the fractional-order PID controller application for the automatic generation control (AGC) application.

One option is using the evolutionary algorithm to solve the LFC problem. The primary goal of EA is for them to be able to manage nonlinear functions [21]. EA applications include equilibrium optimization [20], particle swarm optimization [22], equilibrium optimization technique [23], bacteria foraging optimization [24], grey wolf optimization [25], cuckoo search algorithm [26], bat algorithm [27], gravitational search algorithm [28], and artificial bee colony optimization [29]. LFC design has been successfully implemented using EA. Although these techniques provide a powerful execution and manage a realistic LFC structure, their convergence rate is prolonged and frequently trapped in local optima.

In recent years, another calculation grown prevalently known as the honey badger algorithm (HBA) has been comprehensively used in various optimization issues. The previously mentioned HBA calculation is a population-based technique that starts with a bunch of randomly chosen candidates and helps their improvement estimates through an optimization system [30]. Now, considering all of the previously mentioned factors, a novel approach is made by integrating various renewable energy sources in a three-area AGC system, and a honey badger algorithm (HBA) based on fractional-order PID controller (FOPID) is developed for the load frequency control of the said hybrid power system.

2. Research Gap, Motivation, and Paper Organization

2.1. Literature Review. The observations from the literature reviews can be tabulated as shown in Table 1.

2.2. Research Gap. The main observations obtained from the above literature survey are as follows:

(i) Almost no research has considered the impact of integrating various renewable energy sources into the AGC operation
(ii) To the best of the author's knowledge, the execution of fractional-order PID controller in the distributed power generation-based LFC applications is missing
(iii) profound examination considering different valuable examinations such as variety in sun irradiation, load change, and wind power change has not been accessible in the current studies

2.3. Motivation. The general conclusion of the studied literature is that there are yet many holes that are as yet required to have been tended to for consistent distributed power generation operation. Thus, there is an urgent need to lead a top-to-bottom concentration on frequency support for different parts of distributed power generation applications. Roused from the above realities, a novel approach is made by integrating various renewable energy sources in a three-area AGC system, forming a hybrid power system to investigate the dynamic performances. Likewise, as the hybrid system tuned with a superior improvement technique can guarantee promising outcomes to control complex power systems, a recently seemed honey badger algorithm (HBA) is used to plan a control mechanism for frequency guidelines in distributed power generation operation. The said HBA has been utilized for ideal tuning of the fractional-order PID controller boundaries.

2.4. Paper Organization. The key contributions are quickly depicted as follows:

(i) The advantages of the said algorithm over a few other strategies in terms of execution time and objective function are dissected
(ii) The impact of the coordination of distributed energy within a three-area power system is inspected
(iii) A FOPID controller is arranged with the introduced HBA calculation for the said hybrid system and saw better frequency regulation by differentiating it with some other existing regulators/controllers

The leftover part of this study is coordinated as follows. The subtleties of the test system and numerical modelling of the hybrid system are introduced in Section 3. Section 4 gives the demonstration of the proposed regulator and the used objective function. Section 5 describes a detailed analysis of the HBA optimization algorithm. Simulation results of the further research are introduced in Section 6. Section 7 closes the study.

3. Details of System Understudy

As displayed in Figures 1 and 2, a three-area interconnected hybrid power system involves a thermal power plant unit, a hydroelectric power plant, and other distributed sources such as WTG, PV cell, HAE, PEV, MTG, FC, and DEG in each area. Table 2 [31] shows a lot of nominal gains (K) and time constant (T) limits for the previously mentioned three-area system.

3.1. Modelling of Three-Area Power System Components

(A) Thermal power system: a thermal plant is being utilized to generate power, and the important components are turbine, generator, governor, and reheater with the transfer function as [23]

$$G_t(s) = \frac{K_t}{1 + sT_t}, \tag{1}$$

$$G_P(s) = \frac{K_P}{1 + sT_P}, \tag{2}$$

Table 1: Broad literature review.

References	Key findings	Unsolved issues
[3]	The load frequency control (LFC) problem in a two-area interconnected nonlinear power network	No application of distributed sources into the LFC application
[7]	Fuzzy logic control for LFC of a three-area power system	No application of distributed sources into the LFC application
[20]	Application of modified equilibrium optimization algorithm for LFC of a two-area hybrid power system	Application of distributed sources into the LFC application
[23]	Application of modified equilibrium optimization algorithm for LFC of two-area hybrid distributed power system	Almost no research has considered the impact of integrating various renewable energy sources into the AGC operation

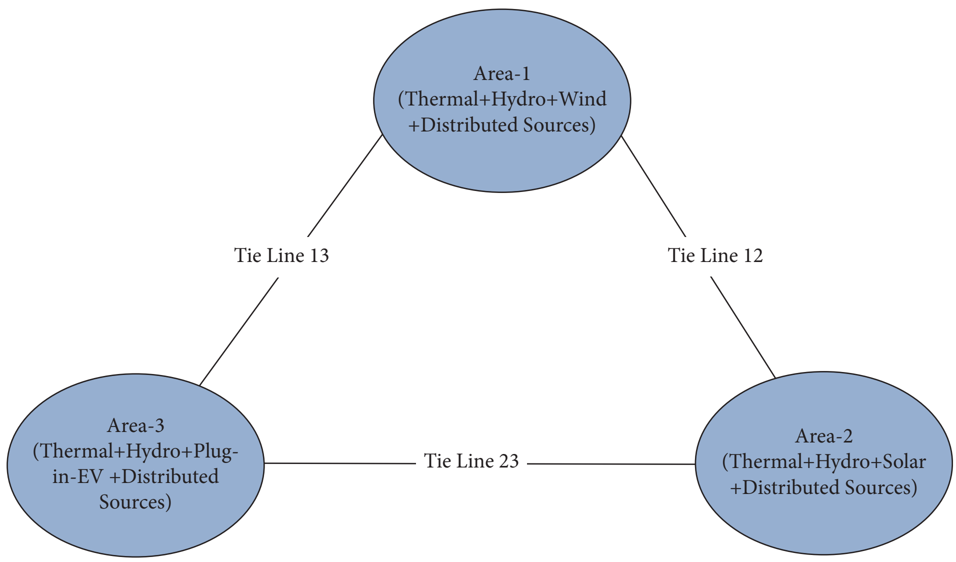

Figure 1: The proposed structure of hybrid three-area power system.

$$G_g(s) = \frac{K_g}{1 + sT_g}, \tag{3}$$

$$G_r(s) = \frac{1 + sK_rT_r}{1 + sT_r}. \tag{4}$$

Equations (1)–(4) represent the transfer function representation of the turbine, generator, governor, and reheater system, respectively.

(B) Hydropower plant modelling: the important components of a hydropower plant are "hydraulic governor" and "hydro turbine" which can be expressed as

$$\begin{aligned} G_{HG}(s) &= \left[\frac{K_1}{1 + sT_1}\right]\left[\frac{1 + sT_R}{1 + sT_2}\right], \\ G_r(s) &= \frac{1 + sT_W}{1 + 0.5 * sT_w}. \end{aligned} \tag{5}$$

(C) WTG system: there are a few nonlinearities in this system that combine pitch angle, and there is a direct relationship between the wind speed and pitch angle, resulting in nonlinearity. Thus, to represent the wind turbine in the low-frequency environment, it can be shown as

$$G_{\mathrm{WTG}}(s) = \frac{K_{\mathrm{WTG}}}{1 + \mathrm{ST}_{\mathrm{WTG}}}. \tag{6}$$

(D) PV system: the PV system comprises a PV module, MPPT tracker, converter, and filter circuit. Numerically, it can be addressed as

$$G_{\mathrm{PV}}(s) = \frac{K_{\mathrm{PV}}}{1 + ST_{\mathrm{PV}}}. \tag{7}$$

(E) Plug-in electric vehicle: a PEV can be defined as a vehicle that draws power from a battery with a limit of basically 4 kW each hour and is fit for being charged from an outside source. PEVs are currently expected to be accused or released of the sensible control plan to take care of the issues brought about by a huge entrance of renewable energy. Thus, the PEV can be expressed as

$$G_{\mathrm{PEV}}(s) = \frac{K_{\mathrm{PEV}}}{1 + sT_{\mathrm{PEV}}} = \frac{\Delta P_{\mathrm{PEV}}}{\Delta U}. \tag{8}$$

(F) HAE system: the HAE is mostly used to take out hydrogen (H2) by utilizing the water electrolysis process and taking care of H2 in the tank after pressure during a typical period. Accordingly, the transfer functions of HAE are addressed by

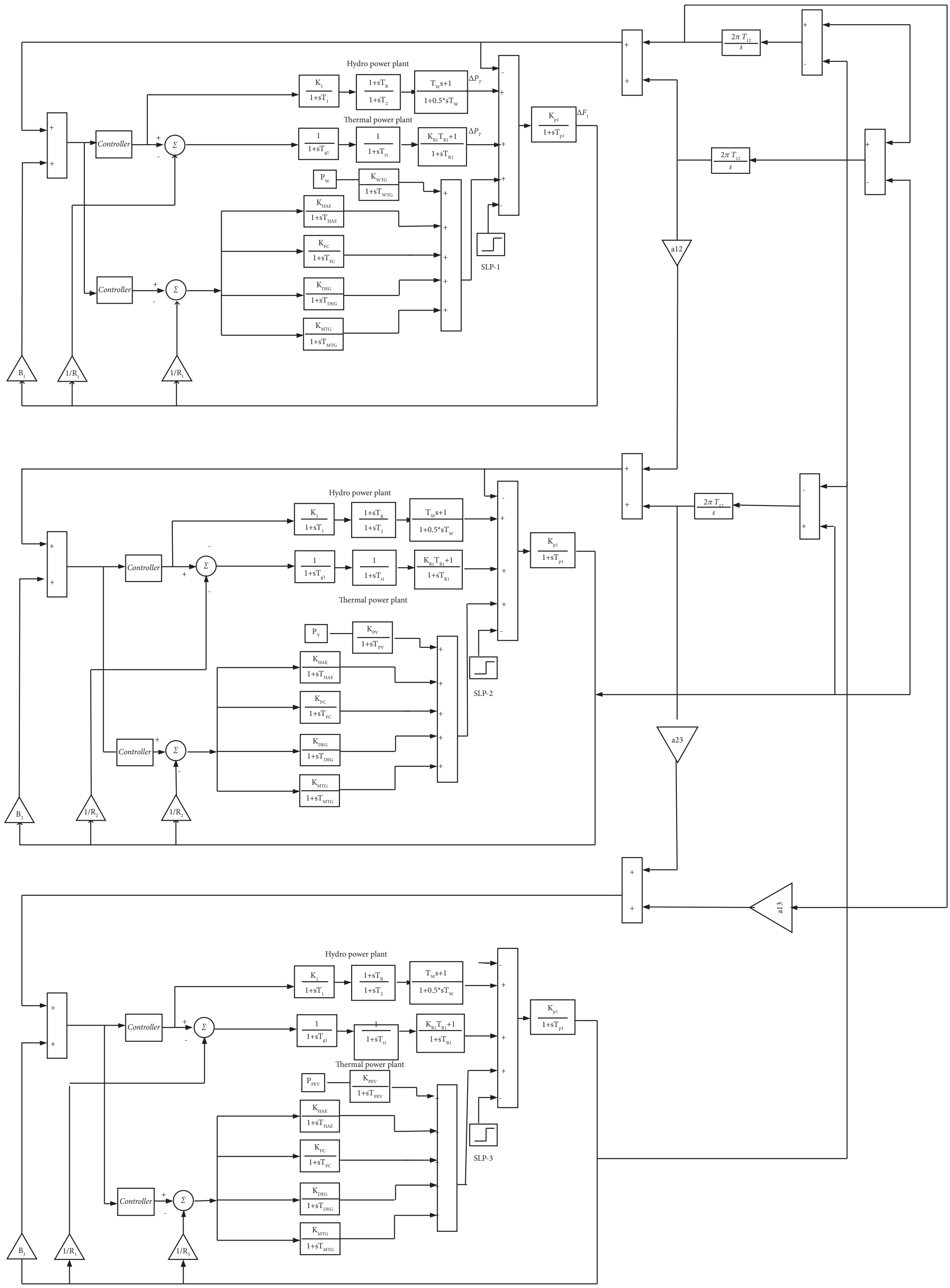

Figure 2: The proposed structure of hybrid three-area power system.

Table 2: Hybrid power system model nominal parameters.

Components	Gain (K)	Time constant (T)
Wind turbine generator (WTG)	$K_{WTG} = 1$	$T_{WTG} = 1.5$
Hydro-aqua electrolyser (AE)	$K_{HAE} = 0.002$	$T_{HAE} = 0.5$
Fuel cell (FC)	$K_{FC} = 0.01$	$T_{FC} = 4$
Diesel engine generator (DEG)	$K_{DEG} = 0.003$	$T_{DEG} = 2$
Microturbine generator (MTG)	$K_{MTG} = 1$	$T_{MTG} = 1.5$
Thermal power station	$K_r = 0.5$, $T_r = 10.0$, $T_{12} = 0.0866$, $B = 0.425$, $T_g = 0.08$, and $T_t = 0.3$	
Hydro power station	$R_1 = 2.4$, $R_2 = 2.4$, $K_p = 120$, $T_p = 20$, $T_2 = 0.513$, $T_R = 5$; $K_1 = 1$, $T_1 = 48.7$, and $T_W = 1$	

$$G_{HAE}(s) = \frac{K_{HAE}}{1 + sT_{HAE}}. \tag{9}$$

(G) FC system: the fuel cell is a crucial part considering its decreased pollution level and expanded productivity which can be expressed as

$$G_{FC}(s) = \frac{K_{FC}}{1 + sT_{FC}}. \tag{10}$$

(H) DEG system: diesel engine generators are expected for giving the absence of power and can restrict the power cumbersomeness among the supply and demand which can be expressed as

$$G_{DEG}(s) = \frac{K_{DEG}}{1 + sT_{DEG}}. \tag{11}$$

(I) MTG system: microturbines, which are also known as mini turbines, can create both power and heat. These turbines, for the most part, have a solitary stage compressor and a solitary stage turbine, with a generator mounted on the same shaft. Numerically, a MTG can be communicated as

$$G_{MTG}(s) = \frac{K_{MTG}}{1 + sT_{MTG}}. \tag{12}$$

(J) Combined power system and load modelling: the power system along with load can be modelled in terms of 1st-order transfer function as

$$G_p(s) = \frac{Kp}{1 + sTp}. \tag{13}$$

4. The Proposed Fractional-Order PID Controller

The generalized transfer function of the FOPID controller can be represented by (1). The other traditional regulators can be effectively acknowledged with the help of this generalized transfer function by picking the suitable values of the variables λ and μ [32]:

$$G(s) = K_p + \frac{K_i}{s^{\lambda}} + K_d s^{\mu}. \tag{14}$$

For instance, by choosing $\lambda = 1$ and $\mu = 0$, proportional integral (PI) regulator can be figured out. Additionally, other ordinary regulators can be acknowledged by picking the suitable values of λ and μ. The FOPID regulator improves the control execution as they give adaptability of control in the full control space instead of a point as on account of traditional PID regulator [33]. In this research work, the FOPID regulator is used as a frequency excursion controller. The FOPID regulator configuration is vital to accomplish acceptable control execution. FOPID regulator is designed with the assistance of the XYZ optimization technique. The structure of the proposed FOPID controller is shown in Figure 3 [33].

4.1. Optimization Problem. In the ongoing examination, the objective is the minimization of frequency deviation by thinking about an integral time absolute error (ITAE) which can be depicted as [34]

$$J = \text{ITAE} = \int_0^{t_{\text{sim}}} \left(|\Delta F_1| + |\Delta F_2| + |\Delta P_{\text{Tie}}| \right) \cdot t \cdot dt, \tag{15}$$

where ΔF_1 and ΔF_2 and ΔP_{tie} and t_{sim} show the area-1 and area-2 frequency deviations and tie-line power deviation and simulation time.

The fitness function and constraints for the above problem is formulated as an optimization problem which are given as

$$\begin{aligned} &\text{Minimize } J \\ &\qquad K_P^R \le K_x \le K_P^S \\ &\text{Subject to } K_I^R \le K_x \le K_I^S \\ &\qquad K_D^R \le K_x \le K_D^S. \end{aligned} \tag{16}$$

5. Honey Badger Algorithm (HBA)

Inspired by the honey badger's clever hunting behaviour, HBA comes up with a more effective search technique for solving many issues that arise in the hard optimization problems. In this algorithm, the two phases, exploration and exploitation, are based on the dynamic search strategy with digging and honey locating method of the honey badger. The detailed steps of the HBA global optimization problem are

Step 1: the number of honey badger of population size N and dimension D is initialized as [30]

$$X = \begin{Bmatrix} K_{11}\, K_{12} \,\ldots\, K_{1D} \\ K_{11}\, K_{12} \,\ldots\, K_{1D} \\ \ldots \\ \ldots \\ K_{N_1}\, K_{N_2} \,\ldots\, K_{\text{ND}} \end{Bmatrix}. \tag{17}$$

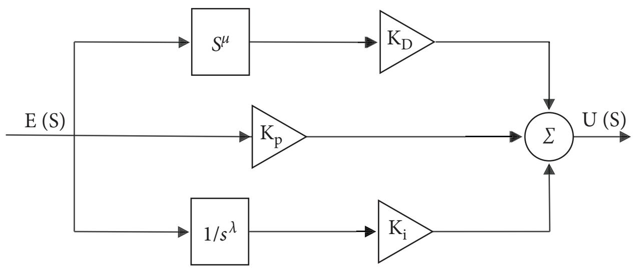

Figure 3: Proposed structure of FOPID controller.

The nth position of X is obtained as

$$x_n = l_{bn} + (u_{bn} - l_{bn}) \times r_1, \tag{18}$$

where l_{bn} and u_{bn} are the lower and upper bound of the search domain of nth position and r_1 is a random number $0 < r_1 < 1$.

Step 2: this step describes the smell intensity in nth honey badger. The strong smell leads to faster motion and vice versa. Hence, I_n is defined as

$$\begin{aligned} I_n &= r_2 \times \frac{C}{4\pi d_n^2}, \\ C &= (x_n - x_{n+1})^2, \\ d_n &= (x_{\text{prey}} - x_n), \end{aligned} \tag{19}$$

where C and d_n represent the concentration strength and distance between the prey and the badger, respectively.

Step 3: the density factor φ is updated with iterations for controlling time-varying randomization as

$$\varphi = c_1 \times \exp\left(-\frac{\text{it}}{\text{IT}_{\max}}\right), \tag{20}$$

where it and $\text{IT}_{\max}$ denote the current and maximum iteration in the algorithm and c_1 is a constant.

Step 4: the two phases in HBA are the digging phase and the honey phase. In the digging phase, x_n is updated as

$$x_{\text{new}}^{G} = \left(x_{\text{prey}} + F_l \times c_2 \times l_n \times x_{\text{prey}} + F_l \times r_3 \times \varphi \times d_n \times \left|\cos(2\pi r_4) \times [1 - \cos(2\pi r_5)]\right|\right), \tag{21}$$

where x_{prey} denotes the global best position, c_2 is a constant. r_3, r_4, and r_5 are random numbers between 0-1, and F_l is known as a flag that helps in exploring the search space while avoiding entering the local optimum:

$$F_l = \begin{cases} 1, & \text{if } r_6 \leq 0.5, \\ -1, & \text{otherwise}, \end{cases} \tag{22}$$

where r_6 is a random number that varies from 0 to 1.

In the honey phase, x_n is updated as

$$x_{\text{new}}^{H} = \left(x_{\text{prey}} + F_l \times r_7 \times \varphi \times d_n\right), \tag{23}$$

where r_7 is a random number [0-1]. At this stage, the new position depends on time-varying density factor φ.

6. Discussion on Simulation Results

6.1. Implementation of Proposed HBA Algorithm. The computation of the objective function for the hybrid power system can be figured out by finishing the simulation by contemplating (17) to track down the limits of the FOPID, PIDF, and PID regulator. Table 3 shows the regulator boundaries which contrast the current strategy with the other standard techniques. It very well might be seen from Table 2 that the HBA-based FOPID controller gives a predominant result when appeared differently in relation to the HBA-based PIDF and the standard HBA-based PID regulator. Likewise, it will overall be pondered that the proposed HBA-based FOPID method gives improved results when veered from PPA. One more perception can be taken from Table 2 that the rate improvement in J with the HBA-based FOPID controller from HBA-based TID, PID, and a conventional GSA-based PID is 5%, 10% and 20%, respectively, consequently supporting the use of the proposed approach. Presently, to test the three-area power system, simulation is done by thinking about the following disturbances.

6.2. Condition 1: Wind Disturbance in Area 1 and Solar Disturbance in Area 2. To exhibit the vigor of the suggested regulator against assortment in electrical power interest, both the areas of the system are presented to self-assertively varying loading design as shown in Figures 4(a) and 4(b). This simulation is done by considering the nominal parameters that appear in Table 1. Figures 5(a) and 5(b) show the reaction of the three-area power system by thinking about the above aggravation. It is noted from Figure 5 that the proposed HBA-based FOPID regulator shows stable execution under discretionarily fluctuating wind and solar patterns.

6.3. Condition 2: Wind Disturbance in Area 1. For the first instant, the proposed distributed energy source-based three-area hybrid power system is attempted with a wind unsettling influence in region 1 as displayed in Figure 4(a). Figures 6(a)–6(c) show the frequency response of region 1 (Δf_1) and region 2 (Δf_2) and tie-line power modification (ΔP_{tie12}) after going through irritation with different

Table 3: Optimized parameters for the hybrid power system.

Parameters	Proposed HBA-tuned FOPID controller	HBA-tuned TID controller	HBA-tuned PID controller	GSA-tuned PID
Controller 1	$K_P = 1.6491$, $K_I = 1.8964$, $K_D = 1.8965$	$K_P = 1.6987$, $K_I = 1.9898$, $K_D = 1.8965$	$K_P = 1.9987$, $K_I = 1.9987$, $K_{D1} = 1.9987$	$K_P = 1.9985$, $K_I = 0.9987$, $K_{D1} = 1.6669$
Controller 2	$K_P = 1.6984$, $K_I = 1.8974$, $K_D = 1.9853$	$K_P = 1.8976$, $K_I = 1.8562$, $K_D = 1.6985$	$K_P = 1.9987$, $K_I = 1.9987$, $K_{D1} = 1.9987$	$K_P = 1.9236$, $K_I = 1.9865$, $K_D = 1.9541$
Controller 3	$K_P = 1.9856$, $K_I = 1.8978$, $K_D = 1.7865$	$K_P = 1.8965$, $K_I = 1.9658$, $K_D = 1.6985$	$K_P = 1.9987$, $K_I = 1.9987$, $K_{D1} = 1.9987$	$K_P = 1.9946$, $K_I = 1.9306$, $K_D = 1.9943$
Controller 4	$K_P = 1.8965$, $K_I = 1.9852$, $K_D = 1.99658$	$K_P = 1.9632$, $K_I = 1.8965$, $K_D = 1.6985$	$K_P = 1.8974$, $K_I = 1.9121$, $K_{D1} = 1.6895$	$K_P = 1.9896$, $K_I = 1.9987$, $K_D = 1.9987$
Controller 5	$K_P = 1.8975$, $K_I = 1.7854$, $K_D = 1.8956$	$K_P = 1.9987$, $K_I = 1.9987$, $K_D = 1.9987$	$K_P = 1.6985$, $K_I = 1.8956$, $K_{D1} = 1.9658$	$K_P = 1.8799$, $K_I = 1.8887$, $K_D = 1.9987$
Controller 6	$K_P = 1.9655$, $K_I = 1.8965$, $K_D = 1.8965$	$K_P = 1.9987$, $K_I = 1.9987$, $K_D = 1.9987$	$K_P = 1.7845$, $K_I = 1.9654$, $K_{D1} = 1.9865$	$K_P = 1.9987$, $K_I = 1.9987$, $K_D = 1.9856$
ITAE	54.6	57.1	59.3	68.03

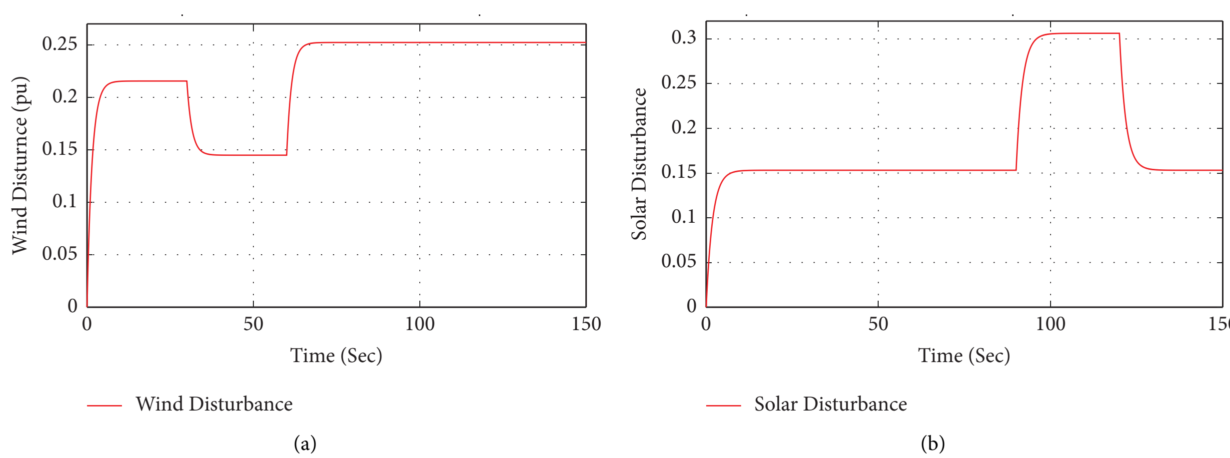

Figure 4: (a andb) Different disturbances of the hybrid power system. (a) Wind disturbance for area 1. (b) Solar disturbance for area 1.

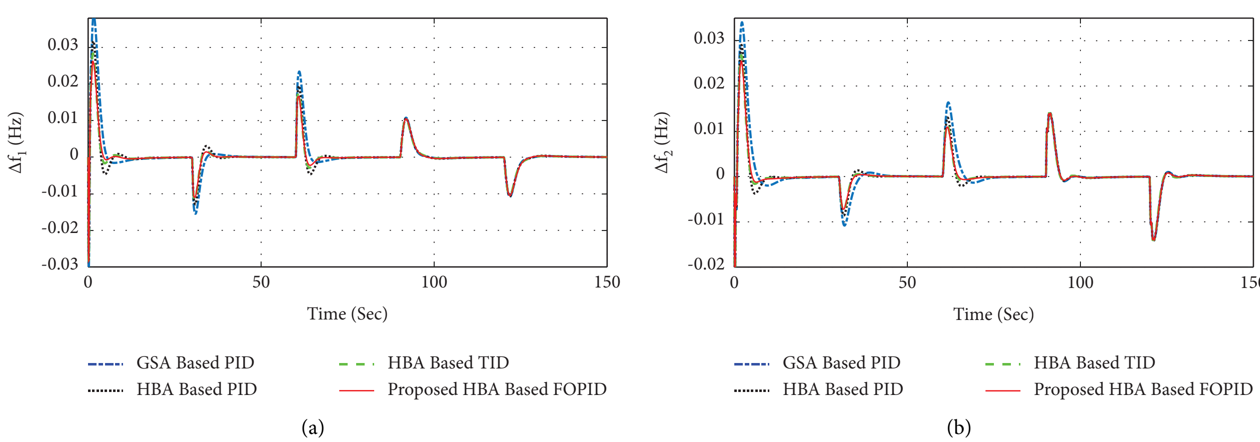

Figure 5: Continued.

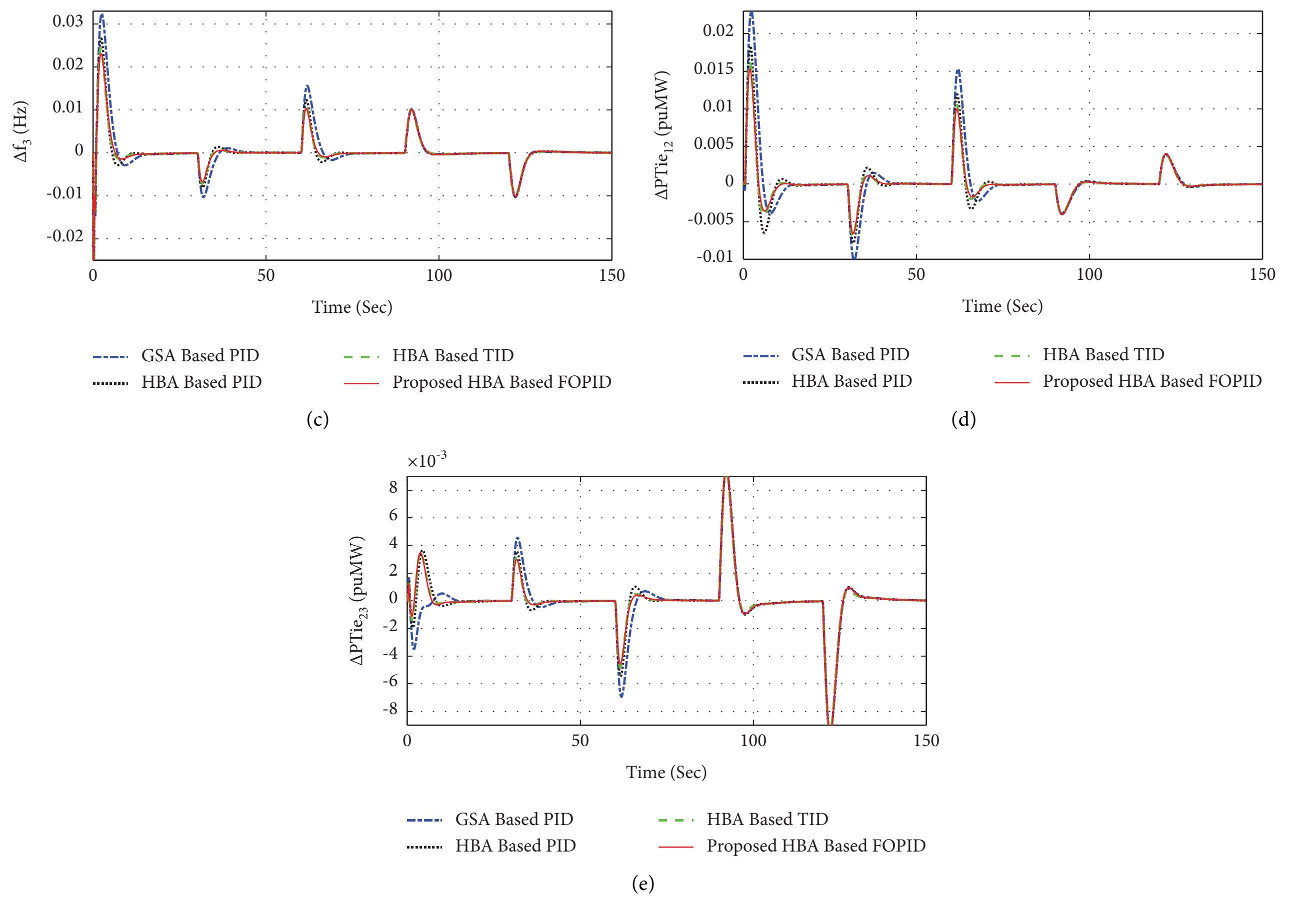

Figure 5: (a–e) System response for condition 1: (a) A_1, (b) A_2, (c) A_3, (d) P_{tie12}, and (e) P_{tie23}.

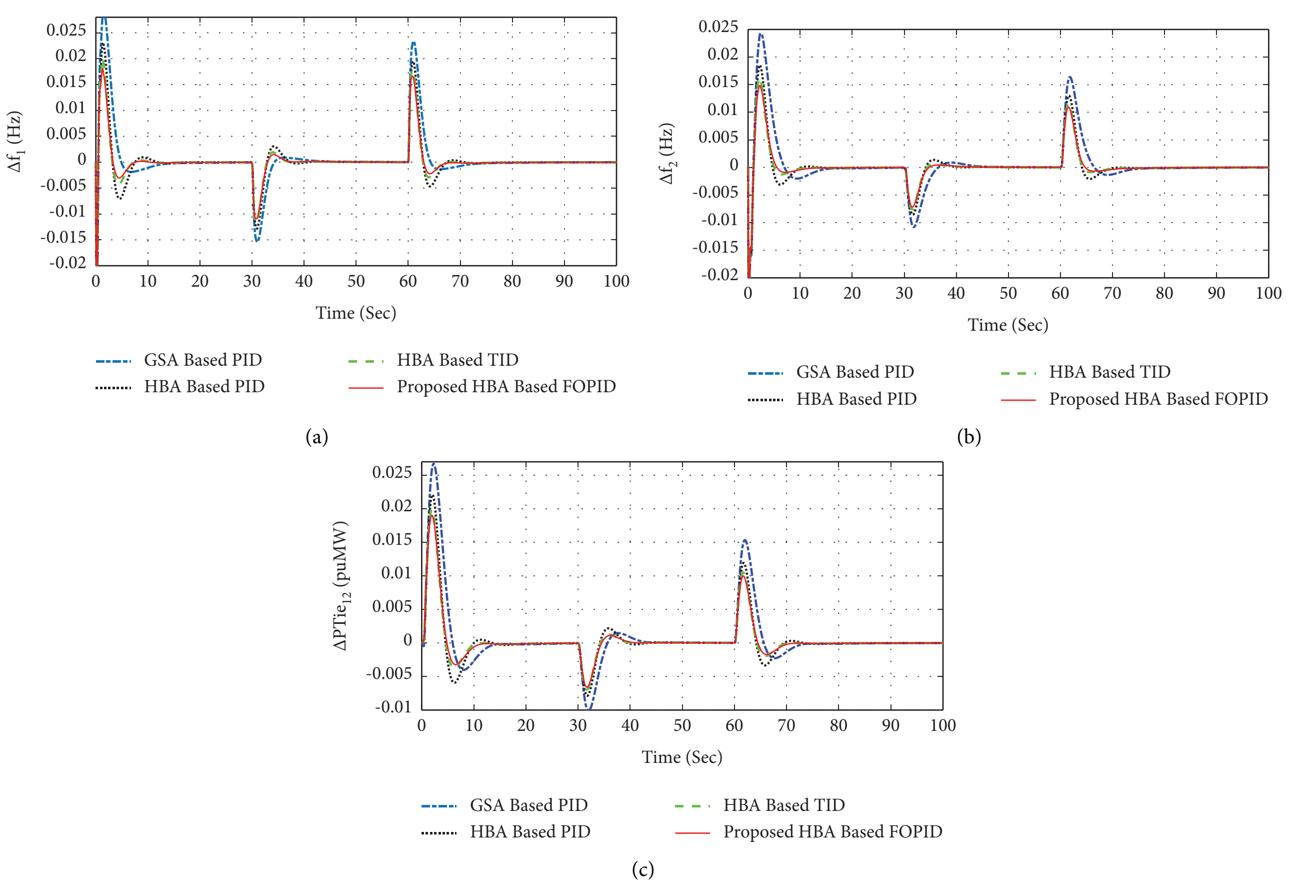

Figure 6: (a–c) System response for condition 2: (a) A_1, (b) A_2, and (c) P_{tie12}.

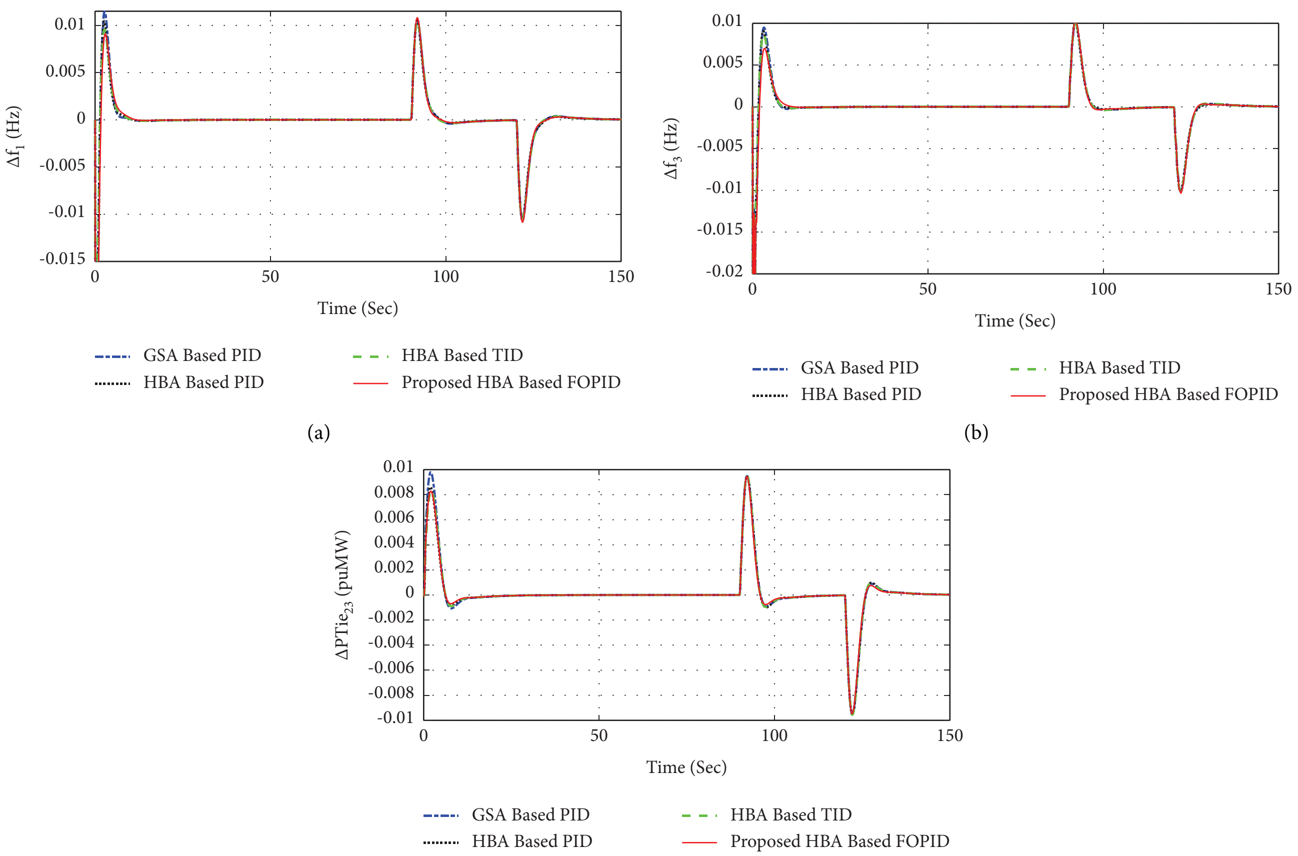

Figure 7: (a–c) System response for condition 3: (a) A_1, (b) A_3, and (c) P_{tie23}.

Table 4: Sensitivity analysis parameters for the hybrid power system.

Parameters	Value
Governor time constant (T_g)	0.16 (+50%)
Turbine time constant (T_t)	0.7 (+75%)
Frequency bias factor (β)	0.34 (−20%)
Droop characteristics (R)	2.25 (−25%)
System damping constant (D)	0.027 (−10%)
System inertia constant (M)	0.12 (−70%)

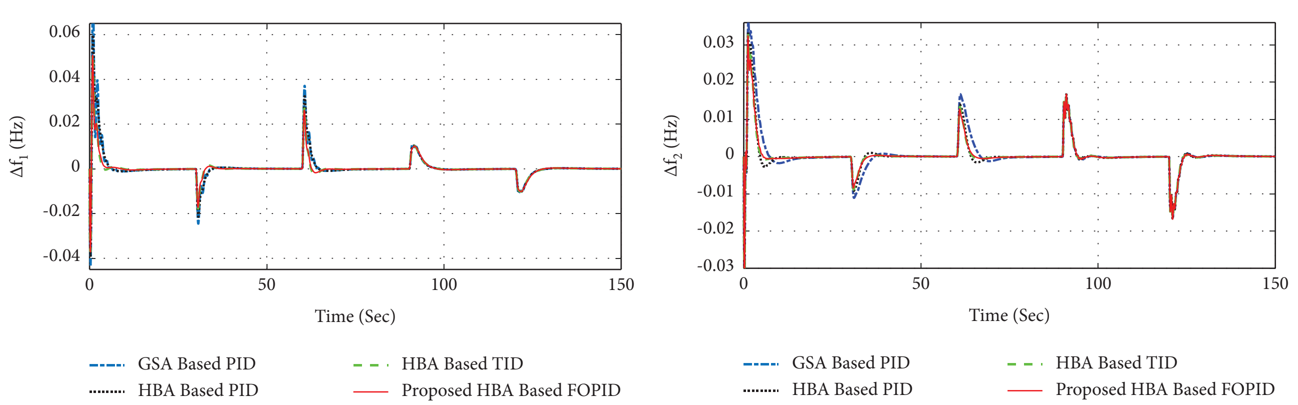

Figure 8: Continued.

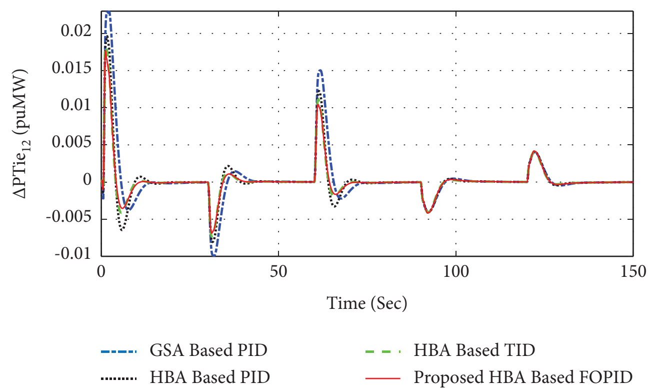

(c)

FIGURE 8: (a–c) System response for sensitivity analysis. (a) A_1, (b) A_2, and (c) P_{tie12}.

proposed controllers. It tends to be seen that there is a calculable contrast between the customary techniques and the proposed HBA-based FOPID regulator.

6.4. Condition 3: Solar Disturbance in Area 2. At the next instant, there is a change in solar power penetration in area 2, as shown in Figure 4(b). Following a similar occasion, the reaction of the three-area system is shown in Figures 7(a)–7(c) as the response in region 1, region 3, and the tie-line power change. A conclusion can be drawn that, after undergoing perturbation, the oscillation of the system can be greatly reduced by the application of the HBA base FOPID controller.

6.5. Condition 4: Sensitivity Analysis of the Proposed Hybrid Power System. At last, a sensitivity investigation is completed to demonstrate the matchless quality of the proposed technique. The said examination is performed by changing the system boundaries as given in Table 4. The proper change of RESs' sources during the said activity is displayed in Figures 8(a)–8(c). It could be seen from the response that real frequency deviations can be doubtlessly taken note of.

7. Conclusion and Future Work

This study proposes a novel honey badger algorithm (HBA) for a FOPID controller structure for frequency control of a hybrid three-area power system. The predominance of the improved algorithm over the standard GSA calculation to the extent simulation time and fitness function is taken immediately. It tends to be seen from the correlation table that there is a high rate of decrease in the performance indices, i.e., in *J* values. The rate improvement in J with the proposed HBA-based FOPID controller contrasted with HBA-based TID, HBA-based PID, and GSA-based PID is 5%, 8%, and 20%, respectively, thus justifying the application of the proposed approach. The HBA approach is then used to design further FOPID controller boundaries for three-area power system frequency regulation. The simulation result demonstrates that the HBA-based FOPID regulator is more productive for frequency regulation than the standard regulator. In the present work, only a few renewable energy sources are included in the hybrid system. Application of some other sources with some different controllers can be tested with some new algorithms in the distributed system which can be considered as a future scope. Its hardware validation can also be considered as a future part of the proposed work.

Data Availability

The figures and tables used to support the findings of this study are included in the article.

Conflicts of Interest

The authors declare that they have no conflicts of interest.

References

[1] O. I. Elgerd, *Electric Energy Systems Theory*, Tata McGraw Hill, New Delhi, India, 2006.

[2] J. Ansari, A. R. Abbasi, and B. B. Firouzi, "Decentralized LMI-based event-triggered integral sliding mode LFC of power systems with disturbance observer," *International Journal of Electrical Power & Energy Systems*, vol. 138, Article ID 107971, 2022.

[3] A. Dev, S. Anand, and M. K. Sarkar, "Nonlinear disturbance observer based adaptive super twisting sliding mode load frequency control for nonlinear interconnected power network," *Asian Journal of Control*, vol. 23, no. 5, pp. 2484–2494, 2021.

[4] B. K. Sahu and P. K. Mohanty, "Design and implementation of fuzzy-PID controller with derivative filter for AGC of two-area interconnected hybrid power system," *International Journal of Innovative Technology and Exploring Engineering*, vol. 8, no. 10, pp. 4198–4212, 2019.

[5] R. K. Khadanga, A. Kumar, and S. Panda, "A novel modified whale optimization algorithm for load frequency controller design of a two-area power system composing of PV grid and thermal generator," *Neural Computing & Applications*, vol. 32, no. 12, pp. 8205–8216, 2019.

[6] M. K. Das, P. Bera, and P. P. Sarkar, "PID-RLNN controllers for discrete mode LFC of a three-area hydrothermal hybrid distributed generation deregulated power system," *International Transactions on Electrical Energy Systems*, vol. 31, no. 5, p. 12837, 2021.

[7] A. Sibilska-Mroziewicz, A. Ordys, J. Możaryn, P. Alinaghi Hosseinabadi, A. Soltani Sharif Abadi, and H. Pota, "LQR and fuzzy logic control for the three-area power system," *Energies*, vol. 14, no. 24, p. 8522, 2021.

[8] A. Latif, D. C. Das, A. K. Barik, and S. Ranjan, "Maiden coordinated load frequency control strategy for ST-AWEC-GEC-BDDG-based independent three-area interconnected microgrid system with the combined effect of diverse energy storage and DC link using BOA-optimised PFOID controller," *IET Renewable Power Generation*, vol. 13, no. 14, pp. 2634–2646, 2019.

[9] I. Pan and S. Das, "Fractional order AGC for distributed energy resources using robust optimization," *IEEE Transactions on Smart Grid*, vol. 7, no. 5, pp. 2175–2186, 2016.

[10] S. Padhy and S. Panda, "Application of a simplified grey wolf optimization technique for adaptive fuzzy PID controller design for frequency regulation of a distributed power generation system," *Protection and Control of Modern Power Systems*, vol. 6, pp. 1–16, 2021.

[11] X. Zhang, T. Tan, B. Zhou, T. Yu, B. Yang, and X. Huang, "Adaptive distributed auction-based algorithm for optimal mileage based AGC dispatch with high participation of renewable energy," *International Journal of Electrical Power & Energy Systems*, vol. 124, no. 124, Article ID 106371, 2021.

[12] E. Celik, N. Ozturk, Y. Arya, and C. Ocak, "(1+PD)-PID cascade controller design for performance betterment of load frequency control in diverse electric power systems," *Neural Computing & Applications*, vol. 33, no. 22, pp. 15433–15456, 2021.

[13] R. Kumar Sahu, S. Panda, A. Biswal, and G. Chandra Sekhar, "Design and analysis of tilt integral derivative controller with filter for load frequency control of multi-area interconnected power systems," *ISA Transactions*, vol. 61, no. 61, pp. 251–264, 2016.

[14] S. Kumari and G. Shankar, "Maiden application of cascade tilt-integral–tilt-derivative controller for performance analysis of load frequency control of interconnected multi-source power system," *IET Generation, Transmission & Distribution*, vol. 13, no. 23, pp. 5326–5338, 2019.

[15] E. Celik, "Design of new fractional order PI–fractional order PD cascade controller through dragonfly search algorithm for advanced load frequency control of power systems," *Soft Computing*, vol. 25, no. 2, pp. 1193–1217, 2021.

[16] D. Guha, P. K. Roy, and S. Banerjee, "Disturbance observer aided optimised fractional-order three-degree-of-freedom tilt-integral-derivative controller for load frequency control of power systems," *IET Generation, Transmission & Distribution*, vol. 15, no. 4, 2021.

[17] E. Cam and I. Kocaarslan, "Load frequency control in two area power systems using fuzzy logic controller," *Energy Conversion and Management*, vol. 46, no. 2, pp. 233–243, 2005.

[18] D. Mukherjee, G. L. Raja, P. Kundu, and A. Ghosh, "Improved fractional augmented control strategies for continuously stirred tank reactors," *Asian Journal of Control*, 2022.

[19] C. Ben Jabeur and H. Seddik, "Design of a PID optimized neural networks and PD fuzzy logic controllers for a two-wheeled mobile robot," *Asian Journal of Control*, vol. 23, no. 1, pp. 23–41, 2021.

[20] R. K. Khadanga, A. Kumar, and S. Panda, "Frequency control in hybrid distributed power systems via type-2 fuzzy PID controller," *IET Renewable Power Generation*, vol. 15, pp. 1706–1723, 2021.

[21] H. H. Alhelou, M. E. Hamedani-Golshan, R. Zamani, E. Heydarian-Forushani, and P. Siano, "Challenges and opportunities of load frequency control in conventional, modern and future smart power systems: a comprehensive review," *Energies*, vol. 11, no. 10, p. 2497, 2018.

[22] C. L. Remes, M. B. Rosa, J. A. Heerdt, and S. V. G. Oliveira, "LQG controller in cascade loop tuned by PSO applied to a DC–DC converter," *Asian Journal of Control*, vol. 23, no. 5, pp. 2370–2380, 2021.

[23] A. Kumar, R. K. Khadanga, and S. Panda, "Reinforced modified equilibrium optimization technique-based MS-PID frequency regulator for a hybrid power system with renewable energy sources," *Soft Computing*, vol. 26, no. 11, pp. 5437–5455, 2022.

[24] E. S. Ali and S. M. Abd-Elazim, "Bacteria foraging optimization algorithm-based load frequency controller for interconnected power system," *International Journal of Electrical Power & Energy Systems*, vol. 33, no. 3, pp. 633–638, 2011.

[25] R. K. Khadanga, A. Kumar, and S. Panda, "A modified grey wolf optimization with cuckoo search algorithm for load frequency controller design of hybrid power system," *Applied Soft Computing*, vol. 124, Article ID 109011, 2022.

[26] T. Cuong-Le, H. L. Minh, S. Khatir, M. A. Wahab, M. T. Tran, and S. Mirjalili, "A novel version of Cuckoo search algorithm for solving optimization problems," *Expert Systems with Applications*, vol. 186, Article ID 115669, 2021.

[27] X. Zhou, F. Gao, X. Fang, and Z. Lan, "Improved bat algorithm for UAV path planning in three-dimensional space," *IEEE Access*, vol. 9, no. 9, pp. 20100–20116, 2021.

[28] Y. Wang, S. Gao, Y. Yu, Z. Cai, and Z. Wang, "A gravitational search algorithm with hierarchy and distributed framework," *Knowledge-Based Systems*, vol. 218, Article ID 106877, 2021.

[29] A. K. Abdul Zahra and T. Y. Abdalla, "Design of fuzzy super twisting sliding mode control scheme for unknown full vehicle active suspension systems using an artificial bee colony optimization algorithm," *Asian Journal of Control*, vol. 23, no. 4, pp. 1966–1981, 2021.

[30] F. A. Hashim, E. H. Houssein, K. Hussain, M. S. Mabrouk, and W. Al-Atabany, "Honey badger algorithm: new metaheuristic algorithm for solving optimization problems," *Mathematics and Computers in Simulation*, vol. 192, pp. 84–110, 2022.

[31] A. Fathy and A. M. Kassem, "Antlion optimizer-ANFIS load frequency control for multi-interconnected plants comprising photovoltaic and wind turbine," *ISA Transactions*, vol. 87, pp. 282–296, 2019.

[32] A. Kumar and G. Srungavarapu, "TLBO-optimized FOPI controller for three-phase Active rectifier using ZDPC technique," *Arabian Journal for Science and Engineering*, vol. 44, pp. 6951–6965, 2019.

[33] D. Izci, S. Ekinci, and B. Hekimoglu, "Fractional-order PID controller design for buck converter system via hybrid Lévy flight distribution and simulated annealing algorithm," *Arabian Journal for Science and Engineering*, pp. 1–19, 2022.

[34] M. Elsisi, "Optimal design of non-fragile PID controller," *Asian Journal of Control*, vol. 23, no. 2, pp. 729–738, 2021.